Observation of the rock slope thermal regime, coupled with crackmeter stability monitoring: first results from three different sites in Czechia (Central Europe)

Ondřej Racek [1,2], Jan Blahůt [2], Filip Hartvich[2]

[1] Charles University in Prague, Faculty of Sciences, Department of Physical Geography and Geoecology, Albertov 6, 128 43, Prague, Czechia

[2] Department of Engineering Geology, Institute of Rock Structure and Mechanics, Czech Academy of Sciences, V Holesovickach 94/41, 182 09, Prague, Czechia

Correspondence to: Ondřej Racek (racek@irsm.cas.cz)

This paper describes a newly designed, experimental and affordable rock slope monitoring system. By this system, three rock slopes in Czechia are being monitored for the period of up to two years. Three instrumented rock slopes have different lithology (sandstone, limestone, and granite), different aspect and structural and mechanical properties. Induction crackmeters monitor the dynamic of joints, which separate unstable rock blocks from the rock face. This setup works with a repeatability of 0.05 mm. External destabilizing factors (air temperature, precipitation, incoming and outgoing radiation, etc.) are measured by weather station placed directly within the rock slope. Thermal behaviour in rock slope surface zone is monitored using a compound temperature probe, placed inside a 3 m deep sub-horizontal borehole insulated from external air temperature. Additionally, one thermocouple is placed directly on the rock slope surface. From so far measured time series (longest one since autumn 2018) we can distinguish differences between the monitored sites annual and diurnal temperature cycles. From the first data, the greater annual joint dynamic is measured in the case of larger blocks, however, smaller blocks are more responsive to short-term diurnal temperature cycles. The differences in the thermal regime between sites are also recognisable, and are mainly caused by different aspect, rock mass thermal conductivity and colour. These differences will be explained by statistical analyses of longer time series in the future. Moreover, we will use radiation and thermal data, to construct numerical models of rock slopes thermal-stress behaviour.

Keywords: monitoring, rock slope, stability, temperature, crackmeter, horizontal borehole temperature

1 Introduction

The rock slope stability is crucially influenced by both rock properties and exogenous factors (D'Amato et al. 2016, Selby 1980). The rock physical properties are well known and numerous laboratory experiments and theoretical works exist in the field, however, there are very few in-situ experiments that would deal with real-world time and space scales (Fantini et al. 2016; Bakun-Mazor et al. 2013, 2020; Janeras et al. 2017; Marmoni et al. 2020; Isaka et al., 2018). Moreover, all these studies are focused on monitoring of a single, well-known unstable rock slope.

Thermal expansion and frost action together with severe rainfall events are the main exogenous physical processes of the mechanical weathering of the rock surface (Krautblatter and Moser, 2009). Together with chemical weathering, these ultimately result into weakening of the rocks slopes and lowering their stability (Gunzburger et al. 2005, Vespremeanu-Stroe and Vasile, 2010; do Amaral Vargas et al. 2013; Draebing 2020). The loss of stability, caused by repeated changes in the stress field inside the rock eventually leads to a rockfall, one of the fastest and most dangerous forms of slope processes (Weber et al. 2017, 2018; Gunzburger et al. 2005). In the alpine environment, rock falls are increasingly caused by permafrost degradation and frost cracking (Gruber et al. 2004; Ravanel et al. 2017) or temperature related glacial retreat (Hoelzle et al. 2017). To address the influence of permafrost melting on the rock slope stability, several monitoring systems/campaigns were proposed. Magnin et al. (2015a) constructed a monitoring system consisting of rock temperature monitoring both on the rock face and in-depth sensors. In-depth rock mass temperature monitoring is placed in up to 10m deep boreholes. The monitoring is coupled with ERT campaigns to determine sensitive permafrost areas (Magnin et al. 2015b). Girard et al. (2012), introduced a custom acoustic emission monitoring system for quantifying freeze-induced damage in rock. Extensive monitoring system for permafrost activity in Switzerland is presented by Vonder Mühll et al., (2008) and Noetzli and Pellet, (2020). Moreover, a significant percentage of small rock falls is directly triggered by rainfall (Krautblatter and Moser, 2009; Ansari et al, 2015). The linkage between rock fall occurrence and rainfall intensity is not linear and the majority of events is triggered when rainfall intensity exceeds a specific threshold.

Among the destabilizing processes caused by changes in rock temperature and contributing to the decrease of stability are:

- rock wedging-ratcheting (Bakun Mazor et al., 2020; Pasten et al., 2015)
- repeated freeze-thaw cycles
- thermal expansion-induced strain (Gunzburger et al., 2005; Matsuoka 2008)
- and in specific conditions, exfoliation sheets can be destabilized by cyclic thermal stress (Collins and Stock, 2016; Collins et al., 2017).

These processes are often repeated many times, thus effectively widening the joints and fracturing the rock.

Rock slope monitoring is one of the common tasks in engineering geology, often used at construction sites (Ma et al. 2020, Li et al. 2018; Scaoni et al. 2018), along roads or railways or to protect settlements. Various approaches are used, with a background in geodesy (Gunzburger et al. 2005; Reiterer et al. 2010; Yavasoglu et al. 2020), geotechnics (Greif et al. 2017; Lazar et al. 2018), geophysics (Burjanek et al. 2010; 2018; Weber et al. 2017, 2018; Coccia et al. 2016; Yan et al. 2010; Weigand et al. 2020; Warren et al. 2013), or remote sensing methods (Sarro et al. 2018; Matano et al. 2015). Most commonly, sensors such as thermometers, accelerometers, inclinometers, visible light or IR cameras, total stations, TLS, GbSAR and seismographs are used to detect potential rock fall events (Burjanek et al. 2010, 2018; Tripolitsiotis et al. 2015; Matsuoka, 2019). These methods are more suitable for monitoring large rock slopes. Tiltmeters, extensometers and other geotechnical devices are usually used to monitor a single unstable block/part of rock slope (Barton et al. 2000; Lazar et al. 2018). To quantify the influence of meteorological variables, weather station should be included within monitoring systems (Macciotta et al.,

65 2015). Rarely, environmental monitoring is supplemented by solar radiation monitoring (Gunzburger and Merrien-Soukatchoff, 2011).

Usually, approaches and sensors are combined. Large rockslides are monitored by Crosta et al., (2017), Zangerl et al., (2010) and Loew et al., (2012) using combination of remote sensing, geodetical network and borehole inclinometer. Experimental monitoring systems aim to develop or test new sensors or approaches (Loew et al., 2017; Jaboyedoff et al., 2004,

70 2011; Chen et al., 2017; Hellmy et al., 2019) or to describe long term processes of rock slope destabilization (Fantini et al., 2016; Kromer et al., 2019; Du et al., 2017). However, these systems are site-specific and installation of a similar system within multiple sites is complicated and often financially demanding.

Thermal observations are often limited to air temperature and/or rock face temperature monitoring only (Jaboyedoff et al. 2011, Blikra and Christiansen, 2014; Marmoni et al. 2020; Collins and Stock, 2016; Collins et al. 2017; Eppes et al.

75 2016). Less commonly, the temperature changes are measured within the rock mass depth (Magnin, et al. 2015a, Fiorucci et al. 2018). Site-specific designed systems are difficult to modify and usually expensive. This brings difficulties into data processing because they are locally biased and cannot be directly compared.

Therefore, an easy-to-modify, modular and affordable monitoring system composed of crackmeters, weather station, solar radiation and compound borehole temperature probe has been designed and tested. With just minor modifications, various

80 rock slope sites can be easily instrumented, allowing to compare data about rock slope temporal behaviour in different settings. Which we are expecting will bring new, much needed data about rock slope stability spatiotemporal development (Viles, 2013).

2 Monitoring methods

The rock slope monitoring methods have recently gone through a massive development concerning precision, accuracy,

85 reliability, sampling rate, and applicability (Tables 1, 2). Even completely new methods were established, for example, unmanned aerial vehicles applications, TLS, etc. This expansion was mostly allowed by the rapid development of corresponding fields of informatics, computation technologies, communication channels and satellite technology applications.

-    Unlike to above-mentioned systems, the monitoring system presented here (Fig. 1,2; Table 1), can be placed at various sites without major modifications. Using common safety rules and methods for working in heights, the

90   system can be placed directly within vertical or even overhanging rock face. Anchoring must be placed within a stable part of the rock slope, which ensures worker´s safety under any circumstances. This monitoring design brings an opportunity to compare results from different locations and observe generally applicable regularities in rock face thermo-mechanical behaviour thanks to the same instrumentation on various rock slope sites. All sensors are calibrated by manufacturer, before are installed on rock slope to provide precise data. The monitoring

95   system (Table 1, Fig. 1) is composed of the following components:

-    a set of automatic induction crackmeters, coupled with dataloggers (Fig. 1) measuring relative block displacement

- a weather station with a set of sensors measuring various meteorological data (Fig. 1), such as air temperature, humidity and pressure (Table 1), and rock slope surface solar radiation balance (incoming/reflected radiation) of the rock face (Fig. 5) using pair of pyranometers

100
- a set of 12 thermocouples placed along a 3 m deep borehole (Fig 2.), carefully insulated between each neighbouring sensor, measuring rock slope temperature in-depth profile

Component	Manufacturer	Accuracy	Resolution	Repeatibility	Measuring range	Max sampling rate	Protection	Operational temperature	Service life	Price
Crackmeter Gefran PZ 67-20	GEFRAN (It)	<0.1 %	0.05 mm	0.01 mm	0-200 mm	N/A	IP67	-30 - 100 °C	>25*10^8 m stroke	300 €
Datalogger Tertium Beacon	Tertium tech. (It)	N/A	N/A	N/A	N/A	<1 sec	IP65	-30 - 60 °C	>5 years	190 €
Datalogger Temp. Sensor	Tertium tech. (It)	0.02 °C	0.01 °C	N/A	-30 - 60 °C	<1 sec	IP67	-30 - 60 °C	>5 years	
Control unit, battery, solar p	FIEDLER (Cz)	N/A	0.00X; 16bit	N/A	N/A	1 min	IP66	-30 - 60 °C	>5 years	
Temperature sensor	FIEDLER (Cz)	0.1 °C	0.1 °C	0.01° C	-50 - 100 °C	1 min	IP66	-50 - 100 °C	>5 years	
Rain gauge SR03 500cm2	FIEDLER (Cz)	0.05 mm	0.1 mm/year	0.1 mm	N/A	50 m. sec	IP66	0 - 60 °C	>5 years	1 650 €
Humidity sensor	FIEDLER (Cz)	0.008 %	<0.1 %/year	0.02 %	0 - 100 %	1 min	IP66	-50 - 100 °C	>5 years	
Atmospheric pressure senso	FIEDLER (Cz)	2 mbar	0.025 mbar	0.1 mbar	300 - 1100 mbar	1 min	IP66	-40 - 70 °C	>5 years	
Pyranometer SG002	Tlusťák (Cz)	10%/day	20 µV/Wm^2	<5%	300 - 2800 nm (0 - 1200 W/m^2)	1 min	IP66	-30 - 60 °C	>5 years	450 €
Borehole temperature sens	FIEDLER (Cz)	0.1 °C	0.1 °C	0.01° C	-50 - 100 °C	1 min	sealed inside	-30 - 60 °C	>5 years	1 150 €
Datastorage/procesing	FIEDLER/SigFox	/	/	/	/	1 hour	/	/	infinite	200 €

Table 1: List of presented monitoring system components, with performance metrics and prices.

All the elements of the system (Table 1) are commercially available at affordable expenses (one site instrumentation
105 costs approx. 5000 Eur), and are easy to replace by even moderately experienced user. Additional costs are drilling works (1-2 000 EUR). Cost of drilling works depends on the site accessibility and rock mass hardness. The price of the specific monitoring system is also affected by the number of used crackmeters and data loggers. On the other hand, system maintenance costs are not higher than 300 Eur per year including data transmission, processing and storage. This makes system ideal to use on multiple sites, without great financial demands. When using the same instrumentation, data from different rock slope sites
110 can be compared and analysed to better understand general rock slope spatiotemporal behaviour.
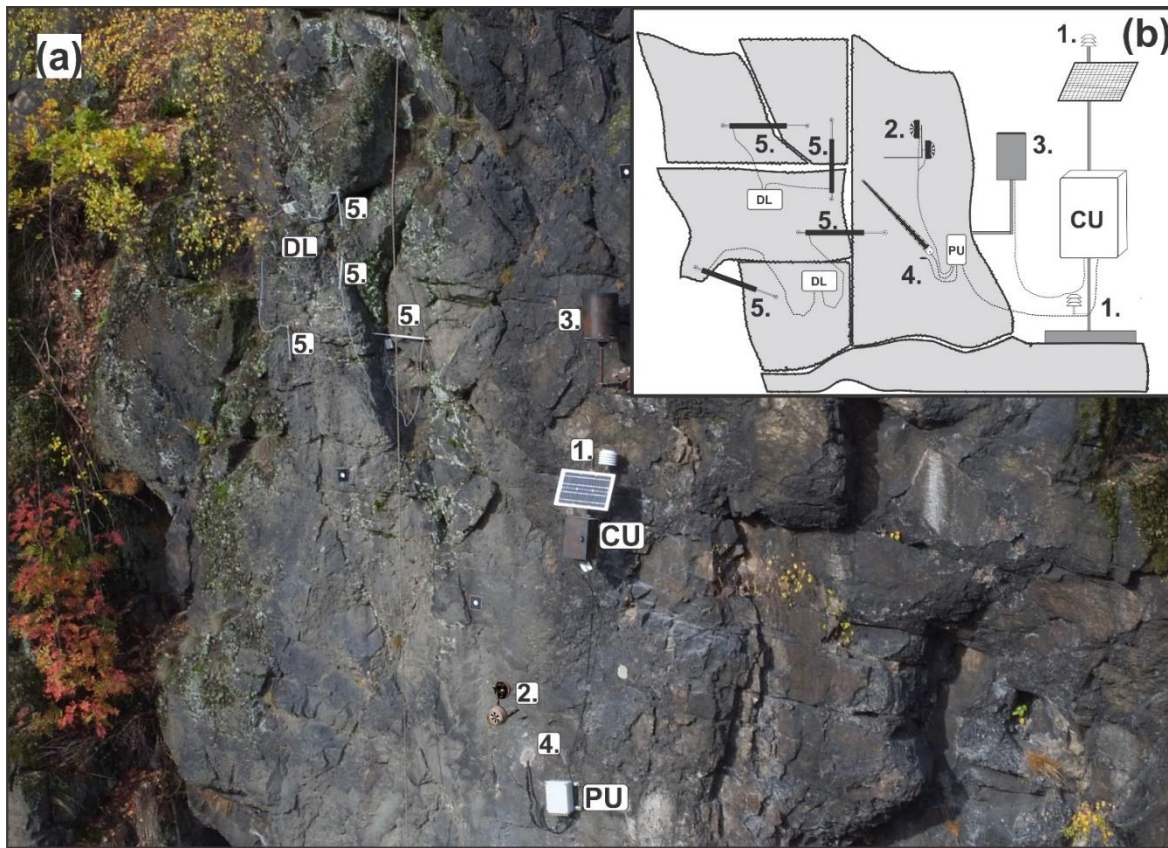
Figure 1: Photo of actual monitoring system at Tašovice site (a). Generalized scheme of the monitoring system (b). CU: control unit, PU: processing unit, DL: data logger, 1.: Temperature sensor, 2.: Pyranometers, 3.: Rain gauge, 4.: Borehole compound temperature probe, 5.: Crack meters (only four of total six crackmeters are visible on this photo)

2.1 Dilatation monitoring

At each site, suitable joints separating unstable rock blocks were selected. Joints and subsequent crackmeter placement were selected to best represent general directions of expected rock blocks destabilization direction. Where it was possible, joints that directly separate unstable block from stable rock were chosen. These joints were afterwards instrumented with calibrated induction crackmeters Gefran PZ-67-200. Crackmeters can record movements smaller than 0.1 mm (Tables 1,2). In comparison with other methods measuring spatial change, their precision is high, with lower costs (Table 2). The temporal resolution of the measurement is nearly continuous when the crackmeter position can be read every second (Table 2). Moreover, we have tested these in a controlled temperature environment using a climate chamber to find out any temperature-dependent errors. In this controlled test, we were able to measure the expansion of a concrete block. The resulting block expansion measurements matched theoretically calculated concrete block expansion. This way we made sure, that measurement of the crackmeters is not biased by dilatation of the device itself. Crackmeters are suitable for harsh conditions (Table 1). Device can stand temperature changes, snow cover, ice accumulation or rainfall with IP 67 protection. These

crackmeters work with good measurement accuracy (Table 1) (GEFRAN, 2019). Crackmeters are coupled with Tertium Beacon dataloggers (Tertium technology, 2019), which also contain accurate in-situ temperature sensors (Table 1). When a datalogger is placed within the discontinuity, records local temperature. The joint dilatation and temperature data are stored in
130   the datalogger and can be wirelessly transmitted at a distance of up to a hundred meters using wi-fi, which simplifies data collection as it can be usually performed from below the rock face. Tertium Beacon data can be sent to a server via IoT SigFox network. The crackmeters and dataloggers are powered with two AA batteries, which last typically 6-12 months according to local climate. The displacement and temperature are set to be measured every hour. This can be however remotely changed if necessary. For example, during special experiments such as thermal camera monitoring campaigns (Racek et al. 2021).
135   Precision of crackmeters allows to monitor small movements in great temporal scale, which cannot be achieved using repeated remote sensing or geodetical campaigns (Table 2).

Method	Results	Range	Precision	Sampling rate	Online data	Price
Induction crack meter	1D distance	< 1 m	0.01 mm	seconds-days	yes	300 €
Precision tape	1D distance	< 30 m	0.5 mm/30 m	hours-days	no	800 €
Fixed wire extensometer	1D distance	10 - 80 m	0.3 mm/30 m	hours-days	yes	4 000 €
Rod for crack opening	1D distance	< 5 m	0.5 mm	hours-days	no	300 €
LVDT	1D distance	< 0.5 m	0.25 mm	seconds-days	yes	170 €
Laser dist. meters	1D distance	< 1000 m	0.3 mm	seconds-days	yes	1 500 €
Portable rod dilatometer	1D distance	< 1 m	0.1 mm	hours-days	no	350 €
Total station triangulation	3D distance	< 1000 m	5 - 10 mm	hours-days	yes	3 000 €
Precise levelling	1D distance	< 50 m	< 1 mm	days	no	350 €
EDM	1D distance	1 - 15 km	1 - 5 mm	minutes - days	no	10 000 €
Terrestrial photog.	3D distance	< 100 m	< 20 mm	hours-days	yes	1 000 €
Aerial photog.	3D distance	< 100 m	10 - 100 mm	days	no	1 500 €
Tiltmeter	inclination change	±10°	0.01°	seconds-days	yes	300 €
GPS	3D distance	Variable	< 5 mm	seconds-days	yes	2 000 €
TLS	3D distance	Variable	5 - 100 mm	hours-days	yes	100 000 €
GB InSAR	3D distance	Variable	< 0.5 mm	hours-days	yes	100 000 €

Table 2: A comparison of rock slope spatial change monitoring techniques (updated after Klimes et al., 2012)

2.2 Environmental monitoring

140   For the monitoring of the weather and climatic parameters at the sites of interest, we use automatic weather stations manufactured by Fiedler environmental systems. These are composed of registration, communication and control unit, external tipping-bucket rain gauge, two temperature sensors, atmospheric pressure sensor, humidity sensor, and a pair of pyranometers, measuring the incoming and reflected solar radiation. All these sensors and the control unit are powered by a 12 V battery, which is charged by a small solar panel (Fig. 1). Except for precipitation, which is measured using a pulse signal, all other
145   meteorological variables and solar radiation are measured every 10 minutes. The control unit is equipped with a GSM modem,

which sends the data automatically to the server of the provider every day. For information about accuracy, durability and price of environmental monitoring see table 1.

To compute the radiation balance (incoming minus reflected solar radiation) of a rock face, it is necessary to measure with two opposite facing pyranometers. For this purpose, a set of pyranometers is used (Gunzburger and Merrien-Soukatchoff, 2011; Janeras et al. 2017; Vasile and Vespremeanu-Stroe, 2017). Pyranometers are placed perpendicular to the rock face, one facing the rock surface while the other the sky hemisphere. This setup enables to measure both incoming and reflected solar radiation. The sensors are not placed directly on the rock face, but on an L-shaped holder, which allows placing both sensors almost at the same point (Fig. 2). The rock-facing pyranometer is placed at a distance of approx. 10 centimetres from the rock surface. The pyranometers have an output of 0–2 V, which corresponds to global radiation of 0–1200 W/m^3, the monitored wavelength spans from 300 to 1200 W/m^2. Monitored wave length spans from 300 to 2800 nm. Outputs from pyranometers are processed by a converter and then sent with the other monitored meteorological variables to the data hosting server.

2.3 Borehole temperature monitoring

For the monitoring of the thermal behaviour of a rock slope, it is necessary to know temperatures at different depths of the rock mass. The newly designed in depth compound temperature probe (Fig. 2) is a crucial part of our monitoring system. The sensors are placed in a 3 m deep sub-horizontal borehole. To ensure safety during drilling and the long lifespan of borehole and sensors, the borehole itself is drilled to the stable part of the rock slope. The borehole is then equipped with a custom-designed probe with a set of thermocouples. Technical parameters of temperature sensors are the same as for air temperature sensors (Tab 1). Thermocouple sensors that are connected to copper rings are originally designed for soil temperature measurement. By connecting these to copper rings, they are suitable to measure temperature of borehole walls. Copper rings with 5 cm diameter are placed at a given distance on the tubular spine (5 cm below the surface, 10 cm, 20 cm, 30 cm, 50 cm, 75 cm, 100 cm, 150 cm, 200 cm, 250 cm and 300 cm). Probe is placed in the sub-horizontal borehole, so copper rings containing temperature sensors lay directly on borehole walls (Fig. 2) By that it is ensured that probe is measuring directly rock mass temperature. Additionally, one thermocouple is placed directly on the rock slab surface (Fig. 2). The head of the borehole is insulated, to prevent air and water inflow into the rock, and the sensors inside the borehole are separated by thorough thermal insulation, to ensure the temperatures are not affected by the air circulation in the borehole. This way, temperature readings from borehole compound probe corresponds with in situ rock mass temperature. The thermal data, collected every 10 minutes, are passed through a converter and send to the main control unit of the environmental station.
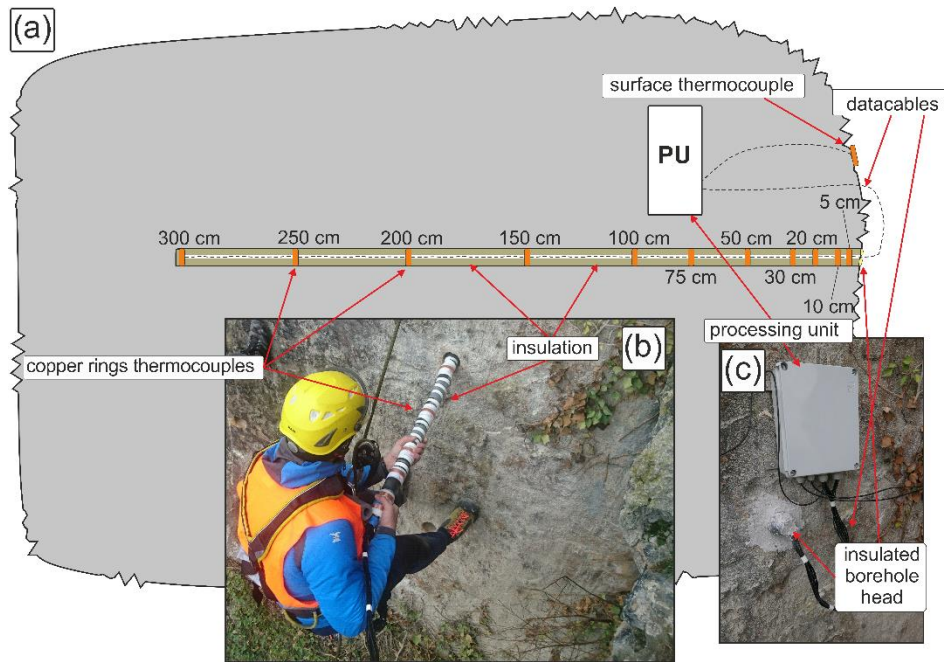
Figure 2: Compound borehole thermocouple probe. (a): generalised scheme, (b): photo of compound thermocouple probe installation, (c): insulated head of sub-horizontal borehole with processing unit.

3 Instrumented sites

The monitoring system has been so far established at three different sites (Fig. 3), using the same instrumentation setup. The sites were chosen deliberately in steep rock slopes built of various rock types, with various aspect, diverse geological history (Fig. 3). To integrate a practical applicability side, locations where the potential rockfall endangers buildings, infrastructure or other social assets were chosen.
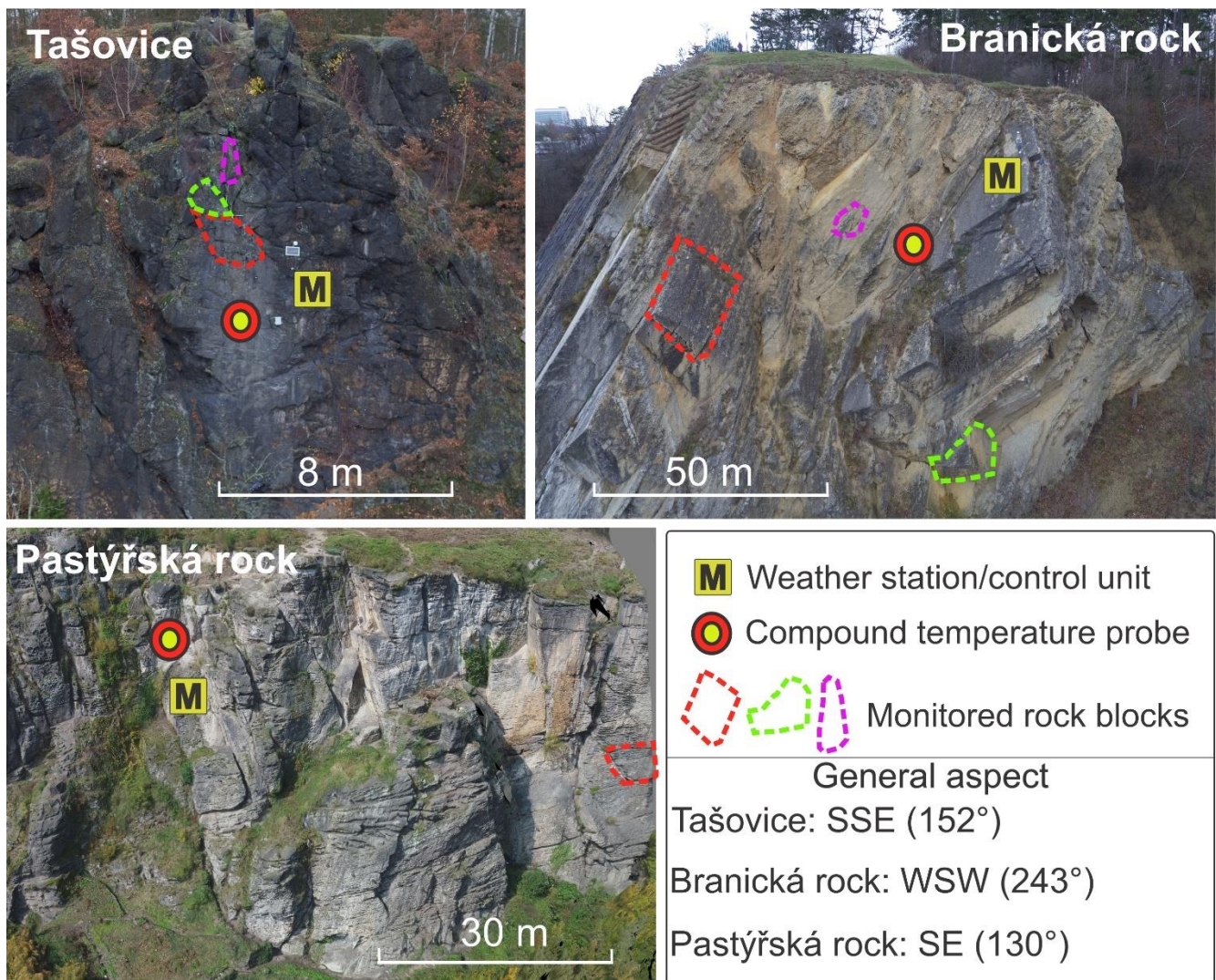
Figure 3: Three instrumented rock slope sites. On each photography are indicated monitored rock blocks (different colour), compound borehole temperature probe and weather station position.

185 **3.1 Pastýřská rock (PS)**

The first instrumented rock slope (Fig. 3) called "Pastýřská rock" is located on the Elbe riverbank in Děčín town, NW Czechia. Monitoring of meteorological variables was started in late 2018 (Table 5.), followed by crackmeters installation and in-depth borehole temperature probe. Pastýřská rock is formed by Cretaceous sandstone, with a general southeast orientation. The mechanical and physical properties of sandstone samples are listed in table 3. The rock slab with pyranometers and borehole is dipping 87° towards the east (085°). On this site, three main discontinuity sets were identified using compass

measurements (Table 4). This locality was known for extensive rock fall activity in past, which lead to rock slope stabilization works in the late 1980s. However, the block monitored by the crackmeters remained in its natural state. At this site, one block is monitored, using two pairs of crackmeters (Table 5). This partial block has dimensions of 6.7 x 10.7 x 2.5 m. The monitored block is located in the overhanging part of the rock slope and all four visible cracks are monitored. The colour of the rock slope surface varies from dark, to light grey (Fig. 3). The rock slab, where the pyranometers are placed is coloured in light grey colour.

3.2 Branická rock (BS)

This rock slope (Fig. 3) in Prague (Central Czechia) was instrumented in summer 2019. This rock slope is formed by several Silurian and Devonian limestone layers, with varying mechanical and physical properties (Table 3). The rock slope was artificially created by blasting and used till the 1950s as a limestone quarry. The rock slope is located on a Vltava riverbank and it is generally facing west-south-westwards. The pyranometers and the borehole temperature sensors are placed on a rock slab dipping 80° to the southwest (235°). Three main discontinuity sets were identified using a geological compass (Table 3). The site was known for extensive rock fall activity in the past, even after quarry closing, which resulted in partial stabilization of known unstable blocks in the 1980s. At this site, three unanchored blocks (Fig. 3) are monitored with seven crackmeters (Table 6). In the upper part of the rock slope lies the largest monitored block at this site, with dimensions 0.9 x 4.5 x 3.7 m. This block is monitored with three crackmeters. The second block is located at the bottom part of the rock slope, partly shaded by vegetation. Dimensions of the second block are 2.5 x 1.6 x 3.6 m. The second block slowly slides on the bottom surface and is instrumented with two crackmeters. Finally, the third monitored block is smaller (0.8 x 1.4 x 0.4 m). It is located in a highly weathered part of rock slope and monitored with two crackmeters. Monitoring at Branická rock site is running since autumn 2019 (Tables 5, 6). The colour of limestone varies from grey to yellow (Fig 3) and the colour of limestone facing pyranometer is light grey.

3.3 Tašovice (T)

The third instrumented site (Fig. 3) is a rock slope above a local road and Ohře river near Karlovy Vary town, west Czechia. Rock slope is formed by partly weathered granite with varying mechanical and physical properties (Table 3). Generally, it is facing south-south-east direction (Fig. 3). The instrumented slab is dipping 88° to the south (170°). At this site, three relatively poorly developed discontinuity systems were identified using a geological compass (Table 3). At this site, small rock falls are frequent as it can be seen from the fresh rock and debris accumulation under the rock face. The locality was fully instrumented with borehole temperature probe, environmental station and global radiation monitoring in spring 2020. Three relatively small blocks are monitored at this site. Block 1 (1.7 x 1 x 2.1 m), Block 2 (0.9 x 0.8 x 0.4 m) and Block 3 (0.5 x 1.2 x 0.4 m). Each block movement is monitored with a pair of crackmeters. The colour of the rock slope varies from black to dark grey. The granite surface at the pyranometers site has dark grey colour (Fig. 3).

4 Fieldwork campaigns

Each instrumented rock slope was characterized using traditional geological, geomorphological and geotechnical methods, such as measuring geometrical properties of joints and fault planes, relative surface strength measurement using a Schmidt hammer, discontinuity density measuring, and stability assessment estimated using geotechnical classifications (Racek, 2020). Mechanical and physical properties of rock samples (Table 3) will serve as inputs to numerical models of thermally induced strain constructed using Multiphysics ELMER (Raback and Malinen, 2016) and FEATool (FEATool, 2017) software.

site	samples	ultrasound testing (wet samples)					pressuremeter (dry samples)					Brazilian test (dry samples)	
		ρ [g/cm^3]	E [GPa]	v [GPa]	v	K[GPa]	hardness [MP	E [GPa]	μ [GPa]	v	K [GPa]	Fmax [kN]	σ_{rt} [MPa]
Pastýřská rock - sandstone	unweathered	1.87 - 1.92	13.8 - 17.4	5.8 - 7.7	0.12 - 0.26	6.6 - 10.4	22.3 - 28.5	14.8 - 17.2	6.2 - 6.9	0.17 - 0.24	7.6 - 11.2	3.0 - 5.5	1.3 - 2.4
	weathered	1.81 - 1.99	8.5 - 15.8	3.7 - 6.3	0.14 - 0.28	4.1 - 11.9	3.9 - 11.0	2.2 - 6.0	1.0 - 2.4	0.24 - 0.39	3.9 - 4.0	0.7 - 3.6	0.3 - 1.6
Branická rock - limestone	unweathered	2.68 - 2.69	75.1 - 79.6	29.2 - 30.8	0.28 - 0.29	58 - 61.9	77.1 - 244.6	65.8 - 75.0	24.9 - 29.0	0.28 - 0.41	50.7 - 129.7	14.1 - 36.1	5.9 - 15.6
	weathered	2.67 - 2.69	73.4 - 78.1	27.9 - 30.2	0.29 - 0.34	62.2 - 64.3	88.2 - 170.5	63.6 - 73.1	24.4 - 28.2	0.27 - 0.31	49.3 - 61.0	18.1 - 33.4	7.8 - 14.0
	with cracks	2.67 - 2.69	64.5 - 78.4	24.4 - 30.3	0.29 - 0.32	60.4 - 63.4	52.1 - 192.3	25.4 - 74.0	9.6 - 27.9	0.27 - 0.33	24.7 - 61.2	11.4 - 26.9	4.7 - 10.9
Tašovice - granite	weathered	2.39 - 2.52	5 - 11.9	1.8 - 4.2	0.39 - 0.42	7.6 - 22.7	36.1 - 63.1	4.3 - 15.0	1.6 - 5.6	0.27 - 0.41	4.4 - 20.4	6.5 - 11.2	2.4 - 5.0

Table 3 Mechanical and physical properties of laboratory tested rock samples from all three monitored sites. ρ: density, E: Young´s modulus, v: Poisson´s ratio, μ: shear modulus, K: bulk modulus, Fmax: maximal axial force, σrt: max tensile strength

Traditional methods were supplemented with state-of-the-art methods of rock slope analysis, including analyses of 3D point clouds and derived mesh surfaces, based on SfM (structure-from-motion, a computerized photogrammetric technique based on the calculation of 3D point cloud from overlapping photos with varying focal axis orientation) (Westoby et al. 2012) processing using the data collected with a UAV or TLS collected data. The obtained detailed rock surface models are then analysed using Cloudcompare and its plugins (Girardeau-Monaut, 2016; Thiele et al. 2018; Dewez et al. 2016) and DSE software (Riquelme et al. 2014) to derive the joint and fault planes and measure their spatiostructural properties (Fig. 4). Discontinuity sets defines partial blocks which forms rock slopes surface.

Discontinuity sets	Pastýřská rock	Branická rock	Tašovice
Systém 1	80/40	50/325	50/090
Systém 2	86/310	90/197	50/220
Systém 3	80/275	62/085	88/345
Systém 4	30/180	62/210	46/181

Table4: Three main discontinuity sets identified in the field using geological compass. Dip/Dip direction
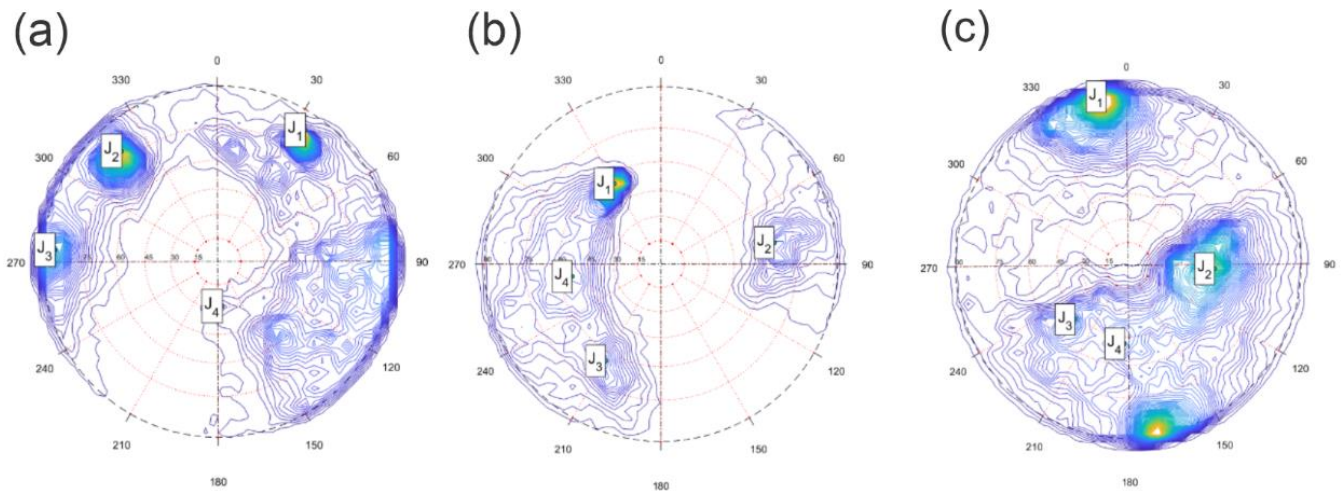
Figure 4: Principal poles density, with four main discontinuity sets (J1 – J4) classified using DSE software (Riquelme et al. 2014). Density of principal poles corresponds to main discontinuity sets identified from point clouds. (a): Pastýřská rock, (b): Branická rock, (c): Tašovice

5 First results

The monitoring systems are operational for 1 to 2 years. During most of the period, the gauges and sensors operated without problems or interruptions. However, some accidents or breakdowns occurred, the most serious being the destruction of one pyranometer by debris, washed down by a rainstorm. As the experimental sites are easy to reach and spare parts easy to obtain, any broken or damaged elements can be replaced within a few days.

From the discontinuity analyses it is visible (Fig. 4, Table 4.), that in the case of Pastýřská and Branická rocks the discontinuity systems are clearly defined. Discontinuity sets are in the case of these sites defined mainly by sedimentary layers and cracks perpendicular to them. In case of Tašovice, discontinuity systems are less pronounced. On this rock discontinuities are linked mainly with tectonically predisposed weak zones and weathered parts of granite rock. Mechanical properties of rock mass samples differ significantly according to degree of weathering (Table 3). Best results in case of hardness were measured for unweathered limestone from Branická rock site. The lowest hardness shows weathered sandstone from Pastýřská rock site. At Tašovice, due to degree of weathering of whole rock slope, we were not able to collect unweathered samples.

5.1 Environmental monitoring

Weather station monitoring on all instrumented sites works without problems. From measured time-series of meteorological variables (Table 5) rock slope microclimate can be defined. From these, the influence of these on the monitored discontinuities position can be determined using statistical analyses. Comparison of crack opening with measured rainfall events using simple graph does not indicate any visible influence of precipitation on the crack opening/closing. However, the measuring period is still short, with prevailing dry, relatively warm weather. Conversely, there is a visible influence of air and rock mass temperature to block dilatation (Racek et al., 2021), where both diurnal and annual cycles can be identified (Fig. 9). Basic statistical data descriptions of measured meteorological variables are listed in Table 5.

Site	Active since	Active days	Rainfall [mm]	Temp. [°C]			Pressure [hPa]			Humidity [%]		
			sum	min	max	mean	min	max	mean	min	max	mean
Pastýřská rock	25.01.18	1098	1503	-9	41.2	10.5	963.5	1026.4	996.9	13.3	96.1	72.9
Branická rock	21.05.19	617	1020	-7	44	13.2	955.3	1017.4	987.4	12.5	95.8	70.4
Tašovice	12.12.18	777	691	-10	45.5	10.4	935.3	997.1	968.8	17.4	96.7	76.4

Table 5: Overview of measured meteorological variables at all three sites. The last measurements considered were measured on 27.1.2021.

5.2 Rock surface radiation balance

Monitoring of rock surface solar radiation balance was installed at monitored rock slopes during 2020 2020 (Branická rock: 1/2020, Pastýřská rock 2/2020; Tašovice 12/2020). Even from these incomplete data we can observe the differences between individual sites (Fig. 5). Local conditions influence incoming radiation pattern by general aspect of the rock slope (temporal shift of incoming radiation peak), rock slope albedo or by shading effect of pyranometer´s surroundings. Differences in the absolute reflected radiation are mainly caused by the different colour of rock faces, and by the different angle of incoming solar radiation caused by the aspect of the instrumented slab.
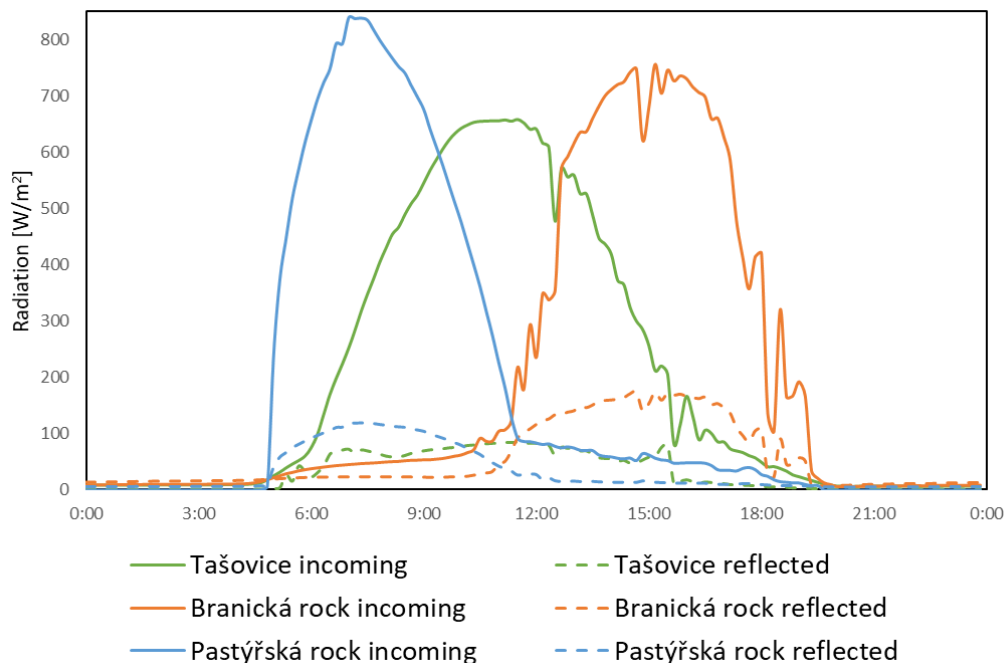
Figure 5: Example of the incoming and reflected radiation measured by pyranometers at Branická rock, Tašovice and Pastýřská rock sites. 24-hour time series of incoming and reflected radiation. Data were recorded 1.8.2020 with no clouds. Influence of slope aspect is obvious from peak incoming radiation shift.

5.3 Borehole temperature

By continuous temperature measuring in different depths inside a sub-horizontal borehole, we can observe both diurnal and annual temperature amplitude in various depths (Fig. 6). In-depth measurements of temperature show differences in temporal thermal behaviour between monitored rock slopes (Fig.6,7). From boxplots that represents data from all monitored sites (Fig 7.), it is visible that largest surface temperature variation has been measured at Tašovice site. This is probably caused by the dark colour of Tašovice rock surface, with lower albedo. However, in greater depths, this variation decreases. This is probably caused by lower thermal diffusivity of the granite. Moreover, in the depth of the rock mass the influence of direct sunlight is attenuated. Greater in-depth temperature variation is present at Pastýřská rock site. However, these data can be biased by different time-series lengths (1 vs 2 full years). Effect of different aspect is visible from peak of diurnal temperature, when on east facing rock slope (Pastýřská rock) temperature peaks earlier then on SSE facing Tašovice and WSW facing Branická rock (Fig. 6). Differences in lithology (different thermal diffusivity) causes temporal shift between surface and subsurface temperature peaks. This temporal shift differs between the different rock slopes. Higher median of the in-depth temperature at Pastýřská and Branická rocks (Fig. 7) is caused by longer in-depth temperature time-series, spanning over two summer periods (Fig. 6).
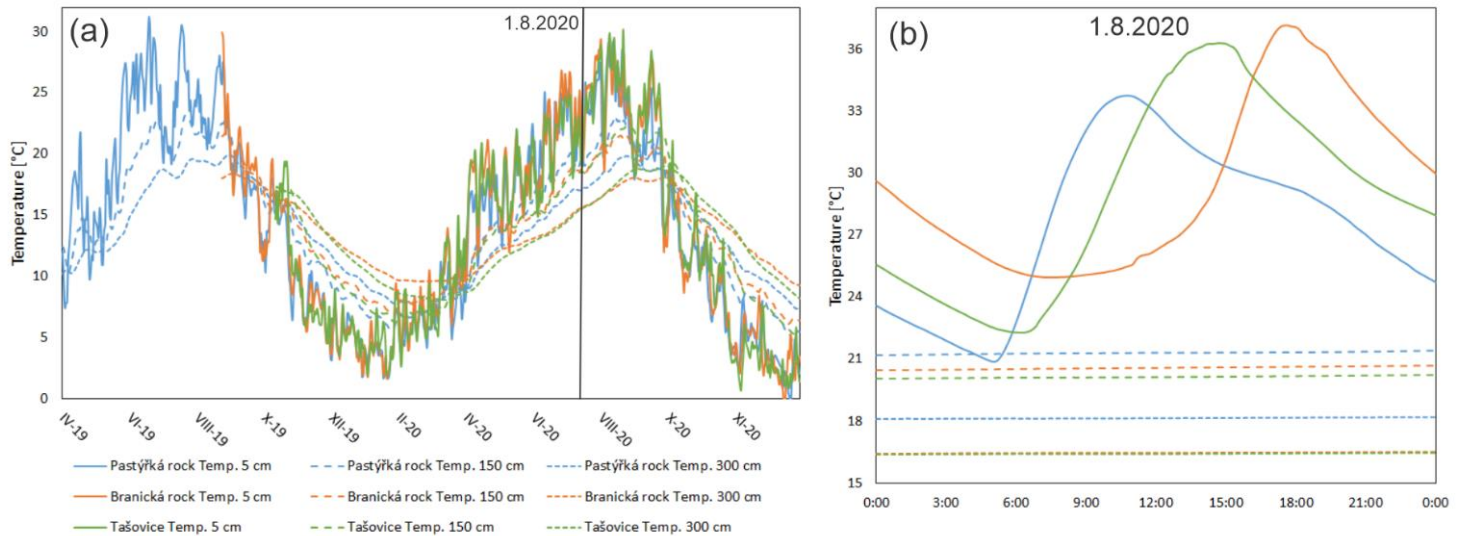
Figure 6: Comparison of temperatures in different rock slope depths (5, 150 and 300 cm) at three monitored rock slopes. (a): long-term data (daily average), (b): one day data from 1.8. 2020
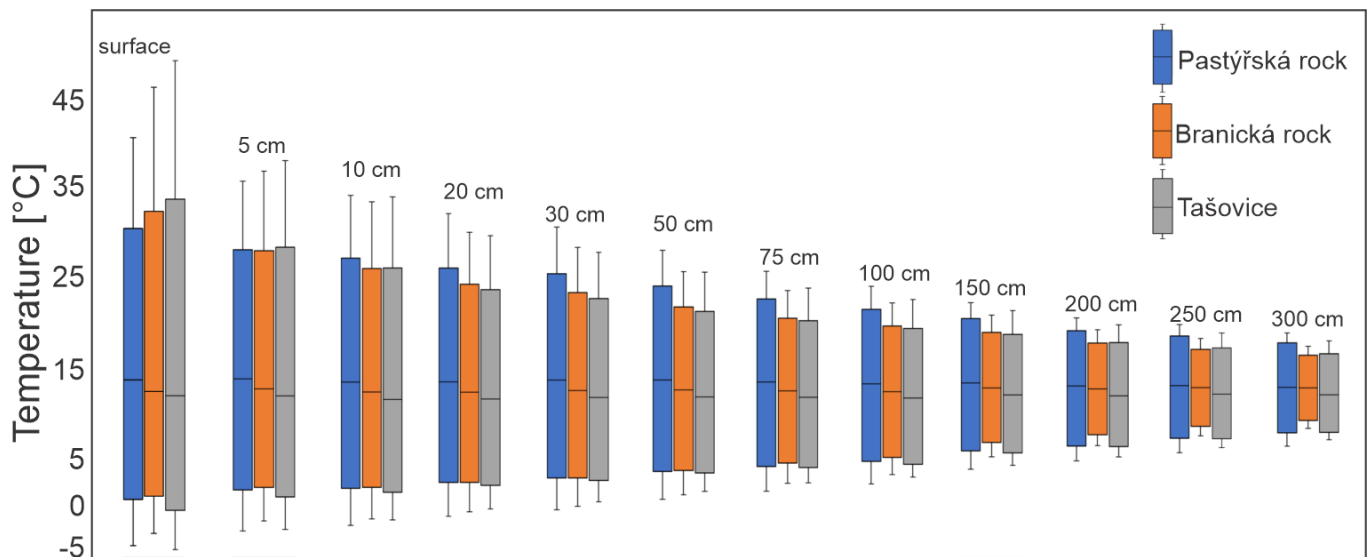
Figure 7: Comparison of in – depth rock mass temperature data from all three monitored sites. Boxplots shows median, minimum, maximum, first and third quartile of temperature data.

5.4 Blocks dilatation

At all monitored sites, the thermally-induced dilatation of individual blocks is observed. However, due to relatively short time-series, the measured crack movements do not yet show any irreversible trends unrelated to air temperature visible on graphs. From the crackmeters data, diurnal and annual amplitudes of crack opening can be identified for all monitored rock blocks. Fig. 9 shows measured diurnal and annual rock crack opening at Pastýřská rock site. From the graph it is visible the

influence of diurnal and annual temperature changes on the crackmeter position. Similar behaviour is observed within all monitored blocks.

The amplitude of crackmeters position differs between individual sites and blocks (Table 6, Fig. 8). These differences are caused by different blocks dimensions, time series length, crackmeters placement and the regime of destabilization.

Site	Block	Crack meter position amplitude Δ l [mm]				measuring since
		CM1-P1	CM1-P2	CM2-P1	CM2-P2	
Pastýřská rock	1	1.05	0.95	0.75	0.75	23.10.18
Branická rock	1	1.45	0.35	0.25	N/A	4.6.19
	2	0.4	0.5	N/A	N/A	20.6.19
	3	0.75	0.7	N/A	N/A	10.7.20
Tašovice	1	0.65	0.25	N/A	N/A	4.12.18
	2	0.6	0.75	N/A	N/A	4.12.18
	3	0.85	0.7	N/A	N/A	18.10.19

Table 6: Amplitude of crackmeters measuring at Pastýřská rock: 1 block 4 crackmeters, Branická rock: 3 blocks 7 crackmeters and Tašovice: 3 blocks 6 crack meters. The table shows the difference between maximal and minimal opening of all placed crackmeters. CM: crackmeter, P: position Last measured data: 27.1.2021

So far, crackmeters amplitudes (Fig. 8, Table 6) higher than 1 mm were measured on Block 1 (approx. 170 m^3) at Pastýřská rock site (PR1_1, PR1_2) and on Block 1 (approx. 16 m^3) at Branická rock site (BR1_1, BR1_2, BR2_1). These blocks are the two largest instrumented. Measured crackmeter amplitude is reversible and thus caused by block thermal expansion/contraction. Relatively small block 3 at Branická rock site (BR4_1, BR4_2) shows movements larger than 0.5 mm although is instrumented only since summer 2020. Such a large amplitude suggests that the block is unstable and by further monitoring this hypothesis should be confirmed.
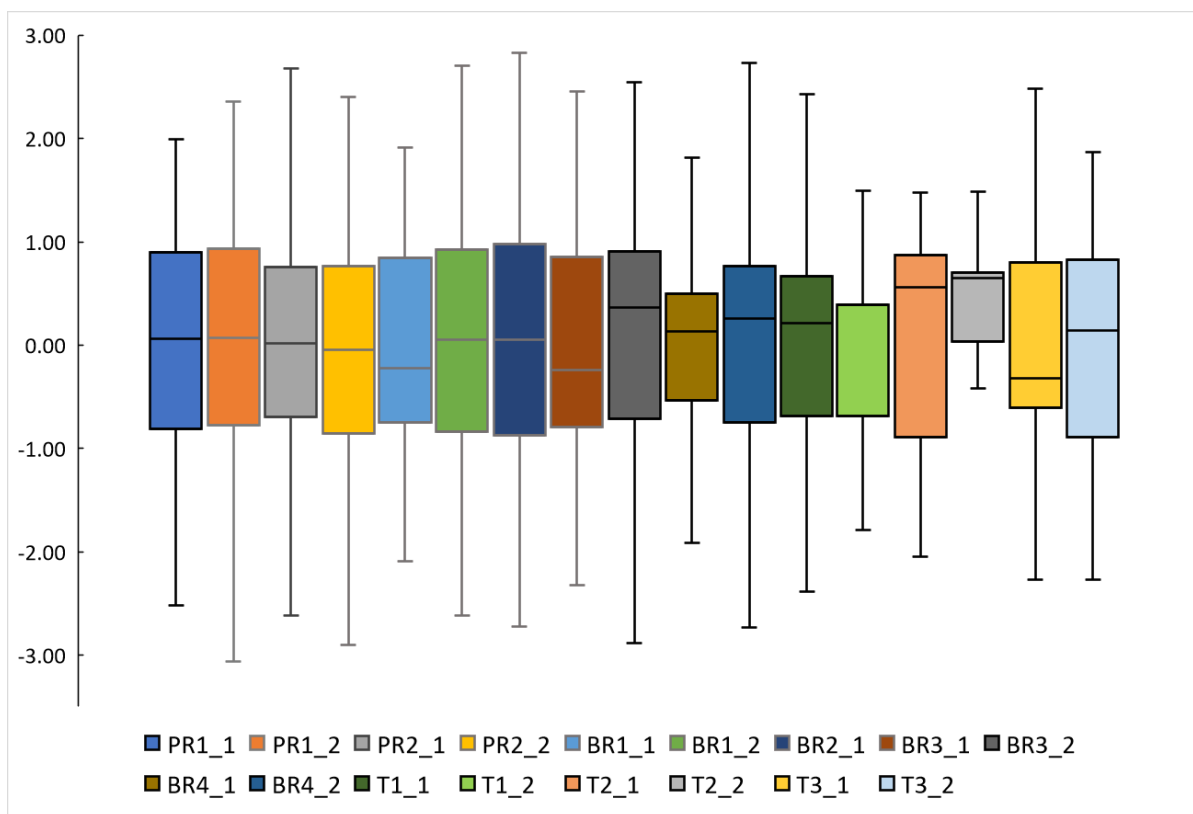
Figure 8: Box plots of crackmeters positions data. To comparison of different positions of measurements, data were standardised. Boxplots shows max/min of crackmeter position, median, first and third quartile.

Blocks that are instrumented at Tašovice site seems to be more stable (Table 6, Fig. 8). Only Block 3 shows 0.85 mm of reversible movement. Again, this block was instrumented at the end of 2019. By further monitoring analyses of crackmeter position graphs and statistical trend analyses possible blocks´ irreversible temperature unrelated trends should be revealed. Destabilization of the single blocks should be visible as irregularities in crackmeter position time-series not strictly related to thermal dilatation. From Table 7. it is visible that two crackmeters at Tašovice site show large amplitude of movement (T2_2, T3_2), however, these movements shown them self's as fully reversible and really short lasting (one-hour measurement). These were probably caused by external forces, such as weight of snow cover deforming crackmeter body or deformation of anchoring point during maintenance. Larger blocks (PR1, BR1; BR2) shows the largest overall amplitude of movements. Rest of smaller blocks shows smaller overall amplitudes however these seem to be more influenced by the short-term diurnal temperature changes. Sensitivity to fast heating/cooling makes these blocks more susceptible to temperature-induced irreversible movements. When data from all crackmeters are standardized (Fig. 8), largest relative dynamic is visible at Pastýřská rock (PR) and Branická rock (BR) blocks. These crackmeters are placed on the two largest monitored blocks. At Tašovice site, dynamic of crackmeters displacement is generally lower.
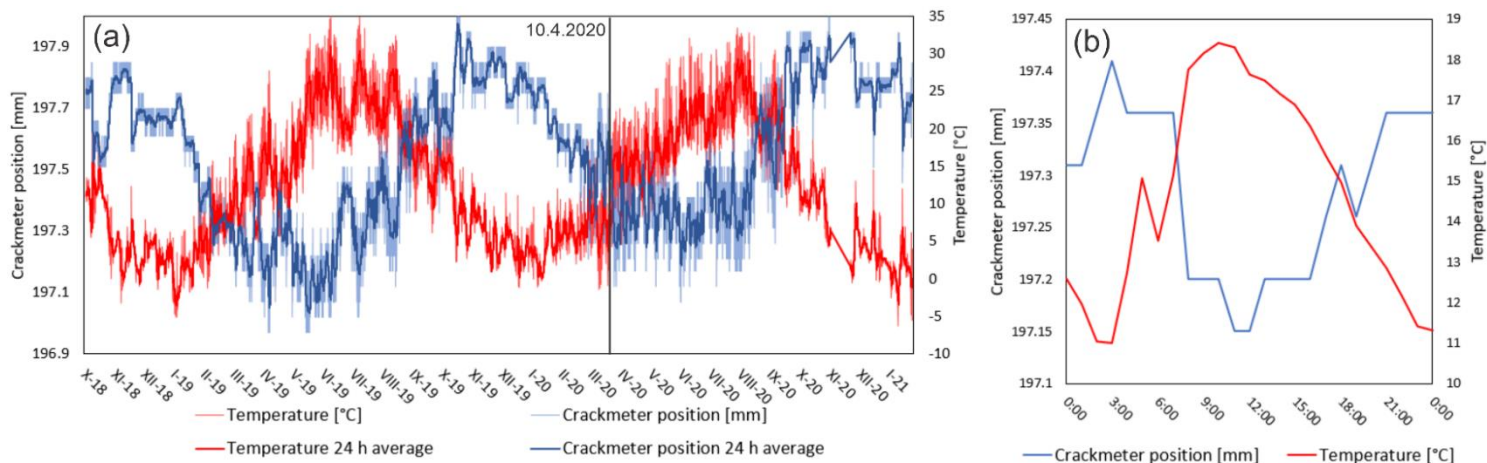
335   **Figure 7: Measured in situ temperature and crack opening at Pastýřská rock site. (a): whole time-series with annual amplitude, (b): example of diurnal amplitude measured on 10.4.2020**

6 Discussion

Commonly used rock stability monitoring systems are often designed to provide an early warning (Jaboyedoff et al. 2004, 2011; Crosta et al. 2017), aiming primarily at the identification of a hazard and not to investigate the causes or thresholds

340   of the movement acceleration. The presented monitoring system is designed to contribute to explaining the various meteorological and temperature related influences on the destabilizing processes, which leads to the eventual loss of rock mass stability and rock fall event triggering (Viles, 2013). Fantini et al. (2017) have concluded that it is the temperature variations (rather than precipitation or wind) that cause changes in internal strain within the rock mass leading to its destabilization. Other factors, such as climate change, former rock fall, seismic stress or hydrological processes are more responsible for rock fall

345   triggering than for short-term strain field modification (Krautblatter and Moser 2009). However, to assess the strain changes within the rock mass, it is necessary to have information on the temperature distribution inside the rock slope depth. This is the crucial advantage of the presented monitoring system, as the borehole temperature compound probe allows to identify short and long-term temperature changes up to 3 m depth.

To observe individual thermally-induced influences of the strain in the rock masses related to air, rock mass

350   temperature and solar radiation, we have placed the monitoring system on rock slopes with various aspect (different insolation and its diurnal and annual changes) and built of different rocks (sandstone, granite and limestone) to include the influence of heat conductivity, capacity and colour of the rock. While there are numerous laboratory studies on rock conductivity (Saez Blásquez et al. 2017), modelling of heat flow based on surface observation (Hall and André, 2001, Marmoni et al. 2020), large-scale experiments usually aiming at heat management in the thermal energy industry (Zhang et al. 2018), only a few

355   experiments have been carried concerning the shallow (first meters) subsurface zone of rock slope (Greif et al. 2017, Magnin et al. 2015a), even though this is the most strained and weathered part of the natural rock mass (Marmoni et al. 2020).

Moreover, thermal conductivity or rock strength can be spatially determined from heating/cooling rates of rock slope surface using thermal camera (Pappalardo et al. 2016; Pappalardo and D'Olivo, 2019; Fiorucci et al. 2018; Guerin et al. 2019). Our approach is aiming to combine these methods, to create simplified numerical thermomechanical models of monitored rock slopes/partial unstable blocks.

The analyses of structural properties of rock were performed using traditional field compass measurements and automatic discontinuity extraction from the UAV SfM photogrammetry produced point clouds using DSE software (Riquelme et al., 2014). While generally, the results were similar, the point cloud analysis did not include discontinuity sets that are not forming the surface of the rock face. This effect is visible mainly in the case of the Tašovice rock slope 3D model, where the structural setting is not so straight forward as it is at Branická rock and Pastýřská rock sites formed by sedimentary layers. Concerning the proposed monitoring system, it is compact, built of cheap and easily accessible off-the-shelf components (Tables 1 and 2), and easy to modify according to specific conditions at rock the slope site. The performance of the monitoring system was so far without major problems. One crackmeter datalogger was damaged and one pyranometer was destroyed by a rockfall triggered by a severe thunderstorm. Otherwise, monitoring works reliably at all instrumented sites. Maintenance is consisting of changing datalogger batteries and cleaning rain gauge buckets. Online data transfer via Sigfox IoT network (crackmeters) and GSM (weather stations) works without problems.

A disadvantage of crackmeter use is that this method provides only one-dimensional spatial change data. On the other hand, this instrumentation is relatively affordable, with good one-dimensional precision and temporal resolution (Table 2). This allows to place multiple crackmeters within one instrumented site. To get full 3D data about an unstable feature´s spatiotemporal behaviour, more crackmeters must be deployed. Additionally, 3D data about larger spatial changes within rock slopes are acquired by UAV SfM photogrammetry and TLS campaigns.

In the case of environmental monitoring, we have found differences between sites (Table 5), caused by aspect and local microclimate. Some differences between sites are caused by different length of meteorological variables time-series (Table 5). When temperature data from in-depth borehole compound probe are compared, differences between monitored sites are apparent (Fig. 6,7). Both diurnal (cca 150 cm depth) and annual temperature cycles (up to 3 m depth) for each site can be defined. Differences between these are caused by the combination of the different aspect of rock slopes and by the thermal behaviour of the different rock types. In further continuation of research, spatial data about rock slope surface temperature will be gained using time lapse thermal camera sensing (Racek et al., 2021). As concerns the weather station and borehole compound temperature probe energy supply, the solar panel is capable of keeping the battery charged even during cloudy weather or snowy winters.

Solar radiation balance is not directly comparable, due to different aspect and slope of instrumented rock slabs. However, the temporal shift in maximum radiance caused by general rock slope aspect is visible from resulted solar radiation data (Fig. 5). When complete annual data about solar radiance will be available in summer 2021, more differences should be found. Then the comparison of long-term solar radiation cycles and theirs influence on rock slope dynamic will be possible.

It is necessary to remark that the destabilisation processes are rather slow and have a low magnitude in the central European mid-latitude climate because of lower temperature amplitude, shorter period of active freeze thaw cycles or lower amount of precipitation (Krautblatter and Moore, 2014; Hermans and Longva, 2012; Viles, 2013). Therefore, long-term time series monitoring is necessary. In addition to these complications, we are preparing installation of monitoring system installation in the Krkonoše Mountains (northern Czechia) at the altitude of 1270 m a.s.l.. In this mountainous environment, block destabilization processes act with greater intensity. Also, there are several cycles with different length, amplitude and depth-reach, ranging from diurnal cycles up to long-term cycles linked with solar activity or climatic oscillations (Gunzburger et al. 2005; Sass and Oberlechner., 2012; Pratt et al. 2019). Among these are the most prominent diurnal and annual cycles (Marmoni et al. 2020). Diurnal cycles have shallower reach (Fig. 6), but are fast and thus cause intensive strain in the surficial rock layer. Annual cycles are slower, but with higher amplitude and depth reach (Hall and André, 2001). In depth temperature data will help to clarify the role of thermally-induced stress in rock disintegration. Temperature changes causes irregular heating and cooling of rock mass. These leads to irregularities in rock mass dilatation at surface and in depth, which causes thermally induced stress/strain, which eventually can lead to discontinuity evolution and breakage of rock mass surface layers. Thermally-driven disintegration also acts at grain scale where grains of different minerals expand differently and induce stresses in to rock mass (Hall and André, 2001;2003).

In combination with the temperature and solar radiation measurements, heat conduction velocity of rock mass can be determined. Diurnal temperature cycles with higher magnitude can play a crucial role in rock fall triggering (Gunzburger et al. 2005; Collins and Stock, 2016). This, together with mechanical properties of the rock mass (Table 3), will allow creating thermomechanical models of the monitored rock slopes in the future. These models, complemented with information on the structural data, mechanical properties of rock mass, IR camera surface temperature and radiation balance of surface measured with pyranometers will help to identify zones where the accumulation of thermally-induced stress concentrates, as the places of potential failure and following destabilization of the rock slope. To calibrate and validate the numerically simulated thermal conductivity, timeseries of in-depth rock mass temperature will be used. Numerical models of partial monitored blocks dilatation and thermally induced stress field changes will follow.

On all sites, the highest diurnal measured crackmeter movements are recorded in the spring and autumn months, when diurnal rock slope surface temperature changes have the largest magnitude. These conditions when the temperature at night falls 0°C and during daytime again rises, are crucial to freeze-thaw cycles development and consequent destabilization of the rocks. We are expecting that irreversible crackmeter position trends will accumulate during these periods.

Several works that use similar monitoring instrumentation and approaches were published (Matsuoka 2008; Bakun-Mazor et al. 2013,2020; Dreabing, 2020; Draebing et al. 2017; Nishi and Matsuaoka 2010). Despite that, thermally induced rock mass deformations monitoring is still relatively marginally studied field. Matsuoka (2008) presented long-term data of crackmeter monitoring. His data were collected on rock slopes in high mountainous alpine environment. Similarly, to our results joint dynamic presented by Matsuoka (2008) is influenced by in-situ air and rock mass temperature. Measured dynamic of monitored joints is highest in spring and autumn, which also corresponds with ours results. From relatively long crackmeter

timeseries Matsuoka (2008) defined gradual, temperature-driven joint opening. Most significant Most significant changes in crackmeter position are explained by freeze-thaw conditions. Nevertheless, even in dynamic alpine environment, joint opening is slow, spanning approx. 0.4 mm in two years of continuous monitoring. It is expected, that in temperate climate these processes are even slower. Nishi and Matsuaoka (2010) described influence of temperature to large rock slide temporal displacement. In this, to our sites different, destabilization mode and mechanism, they have measured large displacement over one meter in three years of monitoring. Movement accelerations were documented during highest precipitations periods. Due to different structural setting and spatial scale of monitored rock slope parts these results are incomparable. Bakun-Mazor et al. (2013, 2020) proposed monitoring system to distinguish thermally and seismically induced joint movements in limestone and dolomites a Masada cultural heritage site. Measured amplitude of thermally-induced irreversible joint movements reached approx. 0.3 mm in one year. With these data, they have described concept of thermally-driven wedging-ratcheting mechanism. Estimated annual irreversible joint opening at Masada was approx. 0.2 mm. In this study, thermally-induced irreversible movements are combined with seismically-induced movements that have higher magnitude.

We assume, that in long-term (several years), we will be able to observe similar wedging-ratcheting mechanism with lower amplitude at our sites. During colder periods, this mechanism can be supported with frost shattering.

Draebing et al. (2017) and Draebing (2020) monitored crack opening in alpine environment. In this extreme environment, they were observed ice wedging driven crack opening up to 1 mm in several days during snowmelt period. By comparing in situ crackmeter temperature and crackmeter opening they have established linkage between in situ temperature and joint dynamic. In their paper joint dynamic is also influenced by snow cover. Measured gradual irreversible joint opening is approx. 0.1 mm/year. Our data from 2020/21 winter period and from newly instrumented site at Krkonoše mountains should show similar results. However, with lack of active permafrost and permanently ice-filled joints at our sites, these movements should have lower magnitude.

Measuring temperature of dry unfrozen rock mass depth is still rarely used approach. measured in depth rock mass temperatures in surface permafrost rock mass zone (Magnin et al. 2015a; Fantini et al. 2018). Magnin et al. (2015a) measure rock mass temperature inside 10 m deep boreholes. This research is oriented mainly to active permafrost depth estimation and its spatiotemporal behaviour. In shallow subsurface zone, they have measured annual temperature amplitude approx. 5°C in 3 m depth. Our data from sub-horizontal boreholes show rock mass temperature amplitude of approx. 10°C in the depth of 3 m. This is probably caused by different climatic setup of ours sites.

 Fantini et al. (2018) studied short-term temperature profiles at experimental limestone quarry rock slope. Diurnal temperature cycles in their case reached maximum depth of approx. 20-30 cm. These results correspond with our measurements. We are able to observe diurnal temperature cycles up to 50 cm depth during summer period, when rock mass surface is intensively heated by solar radiation. It is necessary to mention, that comparison of these results is not straight forward due to diverse climatic setup.

Currently, the three sites are continuously measuring for a period between 1 and 2 years (Table 5). Based on this, we can show that the system is capable of observing the influence of thermal stress to the response of the monitored blocks (Fig.

9). However, to exclude seasonality, the time-series of the crackmeters positions should be longer than 2-3 years. In a longer period, we expect to observe the process of long-term rock slope destabilization represented by a gradual irreversible trend of crack opening/closure, which points on to the partial block destabilization. Longer time series also allow to use seasonal statistical trend tests to describe trends in monitored joints dynamic. The influence of meteorological variables on the rock blocks stability will be statistically analysed, to find out how individual meteorological variables influence dynamic of joints. In-depth temperatures will be analysed to find differences in thermal conductivity, diffusivity and seasonal temperature trend between the monitored sites. Differences in thermo-mechanical behaviour of different rock slopes will be studied using numerical modelling. Furthermore, monitoring system will be continuously upgraded. Installation of in-situ strain gauges monitoring is planned to directly observe changes in rock mass surface strain.

7. Conclusions

A newly designed rock slope stability monitoring system was introduced. The presented monitoring system combines monitoring of meteorological variables with 3 m deep in-rock thermal profile and dilatation of the unstable rock block joints. It brings a unique opportunity to observe long-term gradual changes within the rock face, leading to the rock slope destabilization.

The design of the system allows an easy installation at various locations without major adjustments or changes. All components of the system are available off-the-shelf, at a relatively low price and are easy to replace with low skill requirements. The environmental data are transferred via GSM to a remote server, and the dilatation data are sent via IoT SigFox network or can be downloaded remotely from several tens of meters. Thus, the maintenance visits of the sites can be limited to several months' interval.

The monitored sites are easily comparable as identical monitoring set-up and equipment is used. Thus, we are monitoring the reaction of various rock types on a certain climatic event and observing the differences and similarities on particular sites. This concerns not only movements or expansion of the rock mass but also the heat advance into the rock, its velocity and amplitudes, otherwise very difficult to measure. Significant differences in shallow surface rock mass zone are observable from 3 m borehole thermocouple probe data.

Further development of this project should include the installation of in-situ rock surface strain monitoring using in situ placed strain gauges. In following research, in situ gained data will be used for heat flow and heat-induced strain numerical modelling within the rock mass.

Measuring of joint movements combined with temperature and other external influencing factors will be analysed to understand contribution of individual processes, leading to rock slope destabilization Whole system will be gradually maintained and placed at more suitable sites.

Data availability

490   Data available: https://data.mendeley.com/datasets/4t38tvb4yn/draft?a=f9020d9b-fbd3-4489-a1ca-0e4ffd623212

Authors contribution

O. Racek, J. Blahůt and F. Hartvich designed system and directed instrumentation of sites and continuously processing data and maintain monitored sites

O. Racek processed crack meters data

495   J. Blahůt processed in depth temperature data and environmental data

F. Hartvich supervised all works, helped with graphic parts of manuscript and participated at setting up of the monitoring

Competing interests

"The authors declare that they have no conflict of interest."

8 Acknowledgements

500   This research was carried out in the framework of the long-term conceptual development research organisation RVO: 67985891, TAČR project number: SS02030023 "Rock environment and resources" within program "Environment for life", internal financing from Charles University Progress Q44 and SVV: SVV260438 and the Charles University Grant Agency: GAUK 359421

505   **8 Acknowledgements**

This research was carried out in the framework of the long-term conceptual development research organisation RVO: 67985891, TAČR project number SS02030023 "Rock environment and resources" within program "Environment for life", internal financing from Charles University Progress Q44 and SVV (SVV260438) and the Charles University Grant Agency [GAUK 359421]

510

References

Ansari, M.K., Ahmed, M., Singh, T.N.R., Ghalayani, I., 2015. Rainfall, A Major Cause for Rockfall Hazard along the Roadways, Highways and Railways on Hilly Terrains in India, in: Engineering Geology For Society And Territory - Volume 1. pp. 457-460.

Bakun Mazor, D., Keissar, Y., Feldheim, A., Detournay, C., Hatzor, Y.H., 2020. Thermally-Induced Wedging–Ratcheting Failure Mechanism in Rock Slopes. Rock Mech Rock Eng 53, 2521-2538.. https://doi.org/10.1007/s00603-020-02075-6

Bakun-Mazor, D., Hatzor, Y.H., Glaser, S.D., Santamarina, J.C., 2013. Thermally vs. seismically induced block displacements in Masada rock slopes. Int J Rock Mech Min (1997) 61, 196-211.. https://doi.org/10.1016/j.ijrmms.2013.03.005

Barton, M.E., McCosker, A.M., 2000. Inclinometer and tiltmeter monitoring of a high chalk cliff, in: Barton, M. E., And A. M. Mccosker. "Inclinometer And Tiltmeter Monitoring Of A High Chalk Cliff." Landslides In Research, Theory And Practice: Proceedings Of The 8Th International Symposium On Landslides Held In Cardiff On 26–30 June 2000. Thomas Telford Publishing, pp. 127-132.

Blikra, L., Christiansen, H.H., 2014. A field-based model of permafrost-controlled rockslide deformation in northern Norway. Geomorphology (Amsterdam) 208, 34-49.. https://doi.org/10.1016/j.geomorph.2013.11.014

Burjanek, J., Gassner-Stamm, G., Poggi, V., Moore, J.R., Faeh, D., 2010. Ambient vibration analysis of an unstable mountain slope. Geophys J Int180, 820-828.. https://doi.org/10.1111/j.1365-246X.2009.04451.x

Burjanek, J., Gischig, V., Moore, J.R., Fah, D., 2018. Ambient vibration characterization and monitoring of a rock slope close to collapse. Geophys J Int212, 297-310.. https://doi.org/10.1093/gji/ggx424

Coccia, S., Kinscher, J., Vallet, A., 2016. Microseismic and meteorological monitoring of Séchili-enne (French Alps) rock slope destabilisatio, in: 3. International Symposium Rock Slope Stability (Rss2016), Nov 2016, Lyon, France.. pp. 31-32.

Collins, B.D., Stock, G.M., Eppes, M.C., 2017. Progressive Thermally Induced Fracture of an Exfoliation Dome: Twain Harte, California, USA, in: Isrm Progressive Rock Failure Conference, 5-9 June, Ascona, Switzerland.

Collins, B., Stock, G.M., 2016. Rockfall triggering by cyclic thermal stressing of exfoliation fractures. Nat Geosci9, 395-400.. https://doi.org/10.1038/ngeo2686

Crosta, G.B., Agliardi, F., Rivolta, C., Alberti, S., Dei Cas, L., 2017. Long-term evolution and early warning strategies for complex rockslides by real-time monitoring. Landslides 14, 1615-1632.. https://doi.org/10.1007/s10346-017-0817-8

D'Amato, J., Hantz, D., Guerin, A., Jaboyedoff, M., Baillet, L., Mariscal, A.M., 2016. Influence of meteorological factors on rockfall occurrence in a middle mountain limestone cliff. Nat Hazard Earth Sys 16, 719-735.. https://doi.org/10.5194/nhess-16-719-2016

Dewez, T.J.B., Girardeau-Montaut, D., Allanic, C., Rohmer, J., 2016. Facets: A cloudcompare plugin to extract geological planes from unstructured 3d point clouds, in: Int Arch Photogramm Vol. 41, Iss. B5. Prague, CZECH REPUBLIC, pp. 799-804.

do Amaral Vargas, E., Velloso, R.Q., Chávez, L.E., Gusmao, L., 2013. On the Effect of Thermally Induced Stresses in Failures of Some Rock Slopes in Rio de Janeiro, Brazil. Rock Mech Rock Eng 46, 123-134.. https://doi.org/10.1007/s00603-012-0247-9

Draebing, D., 2020. Identification of rock and fracture kinematics in high Alpine rockwalls under the influence of altitude.. Earth Surf Dynam Discuss 1-31.. https://doi.org/https://doi.org/10.5194/esurf-2020-69

Du, Y., Xie, M.-wen, Jiang, Y.-jing, Li, B., Chicas, S., 2017. Experimental Rock Stability Assessment Using the Frozen–Thawing Test. Rock Mech Rock Eng 50, 1049-1053.. https://doi.org/10.1007/s00603-016-1138-2

Draebing, D., Krautblatter, M., Hoffmann, T., 2017. Thermo-cryogenic controls of fracture kinematics in permafrost rockwalls. Geophys Res Lett 44, 3535-3544.. https://doi.org/10.1002/2016GL072050

Eppes, M., Magi, B., Hallet, B., Delmelle,, E., Mackenzie-Helnwein, P., Warren, K., Swami, S., 2016. Deciphering the role of solar-induced thermal stresses in rock weathering. Geol Soc Am Bull128, 1315-1338.. https://doi.org/10.1130/B31422.1

Fantini, A., Fiorucci, M., Martino, S., Marino, L., Napoli, G., Prestininzi, A., Salvetti, O., Sarandrea, P., Stedile, L., 2016. Multi-sensor system designed for monitoring rock falls: the experimental test-site of Acuto (Italy). Rendiconti Online Societa Geologica Italiana 41, 147-150.. https://doi.org/10.3301/ROL.2016.115

555 Fiorucci, M., Marmoni, G.M., Martino, S., Mazzanti, P., 2018. Thermal Response of Jointed Rock Masses Inferred from Infrared Thermographic Surveying (Acuto Test-Site, Italy). Sensors 18, 2221.. https://doi.org/10.3390/s18072221

GEFRAN, 2020. Position Transducers, 1st ed. 25050 PROVAGLIO D'ISEO (BS) ITALY.

Girardeau-Montaut, D. (2016). CloudCompare. *Retrieved from CloudCompare: https://www. danielgm. net/cc*.

Girard, L., Beutel, J., Gruber, S., Hunziker, J., Lim, R., Weber, S., 2012. A custom acoustic emission monitoring system for
560 harsh environments: application to freezing-induced damage in alpine rock walls. Geosci Instrum Meth1, 155-167.. https://doi.org/10.5194/gi-1-155-2012

Greif, V., Brcek, M., Vlcko, J., Varilova, Z., Zvelebil, J., 2017. Thermomechanical behavior of Pravcicka Brana Rock Arch (Czech Republic). Landslides 14, 1441-1455.. https://doi.org/10.1007/s10346-016-0784-5

Gruber, S., Hoelzle, M., Haeberli, W., 2004. Permafrost thaw and destabilization of Alpine rock walls in the hot summer of 2003.
565 Geophys Res Lett31.. https://doi.org/10.1029/2004GL020051

Guerin, A., Jaboyedoff, Michel, Collins, Brian D., Derron, Marc-Henri, Stock, Greg M., Matasci, Battista, Boesiger, Martin, Lefeuvre, Caroline, Podladchikov, Yury Y., 2019. Detection of rock bridges by infrared thermal imaging and modeling. Sci Rep-UK9, 13138-13138.. https://doi.org/10.1038/s41598-019-49336-1

Gunzburger, Y., Merrien-Soukatchoff, V., 2011. Near-surface temperatures and heat balance of bare outcrops exposed to solar
570 radiation. Earth Surface Processes and Landforms 36, 1577-1589.. https://doi.org/10.1002/esp.2167

Gunzburger, Y., Merrien-Soukatchoff, V., Guglielmi, Y., 2005. Influence of daily surface temperature fluctuations on rock slope stability: case study of the Rochers de Valabres slope (France). Int J Rock Mech Min (1997) 42, 331-349.. https://doi.org/10.1016/j.ijrmms.2004.11.003

Hall, K., Andre, M.F., 2001. New insights into rock weathering from high-frequency rock temperature data: an Antarctic study of
575 weathering by thermal stress. Geomorphology (Amsterdam) 41, 23-35.. https://doi.org/10.1016/S0169-555X(01)00101-5

Hall, K., André, M.F., 2003. Rock thermal data at the grain scale: applicability to granular disintegration in cold environments. Earth Surf Proc Land 28, 823-836.. https://doi.org/10.1002/esp.494

Hellmy, M.A.A., Muhammad, R.F., Shuib, M.K., Fatt, N.T., Abdullah, W.H., Abu Bakar, A., Kugler, R., 2019. Rock Slope Stability Analysis based on Terrestrial LiDAR and Scanline Survey on Karst Hills in Kinta Valley Geopark, Perak, Peninsular Malaysia.
580 Sains Malaysiana 48, 2595-2604.. https://doi.org/10.17576/jsm-2019-4811-29

Hermans, R.L., Longva, O., 2012. Rapid rock-slope failures, in: Landslides: Types, Mechanisms And Modeling. pp. 59-70.

Hoelzle, M., Azisov, E., Barnadum, M., Huss, M., Farinotti, D., Hagg, W., Kenzhebaev, R., Kronenberg, M., Machguth, H., Merkushin, A., Moldobekov, B., Petrov, M., Saks, T., Salzmann, N., Schone, T., Tarasov, Y., Usubaliev, R., Vorogushyn, S., Yakovlev, A., Zemp, M., 2017. Re-establishing glacier monitoring in Kyrgyzstan and Uzbekistan, Central Asia. Geosci Inst Meth
585 6, 397-418.. https://doi.org/10.5194/gi-6-397-2017

Chen, T., Deng, J., Sitar, N., Zheng, J., Liu, T., Liu, A., Zheng, L., 2017. Stability investigation and stabilization of a heavily fractured and loosened rock slope during construction of a strategic hydropower station in China. Eng Geol 221, 70-81.. https://doi.org/10.1016/j.enggeo.2017.02.031

Isaka, B.L.A., Gamage, R.P., Rathnaweera, T.D., Perera, M.S.A., Chandrasekharam, D., Kumari, W.G.P., 2018. An Influence
of Thermally-Induced Micro-Cracking under Cooling Treatments: Mechanical Characteristics of Australian Granite. Energies 11,
1338.. https://doi.org/10.3390/en11061338

Jaboyedoff, M., Oppikofer, T., Derron, M.H., Blikra, L.H., Böhme, M., Saintot, A., 2011. Complex landslide behaviour and
structural control: a three-dimensional conceptual model of Åknes rockslide, Norway. Geological Society, London, Special
Publications 351.

Jaboyedoff, M., Ornstein, P., Rouiller, R.D., 2004. Design of a geodetic database and associated tools for monitoring rock-slope
movements: the example of the top of Randa rockfall scar. Nat Hazard Earth Sys 4, 187-196.. https://doi.org/10.5194/nhess-4-187-2004

Janeras, M., Jara, J.-A., Royan, M.J., Vilaplana, J.-M., Aguasca, A., Fabregas, X., Gili, J.A., Buxo, P., 2017. Multi-technique
approach to rockfall monitoring in the Montserrat massif (Catalonia, NE Spain). Eng Geol 219, 4-20..
https://doi.org/10.1016/j.enggeo.2016.12.010

Klimes, J., Rowberry, M.D., Blahut, J., Briestensky, M., Hartvich, F., Kost'ak, B., Rybar, J., Stemberk, J., Stepancikova, P.,
2012. The monitoring of slow-moving landslides and assessment of stabilisation measures using an optical–mechanical crack
gauge. Landslides 9, 407-415.. https://doi.org/10.1007/s10346-011-0306-4

Krautblatter, M., Moser, M., 2009. A nonlinear model coupling rockfall and rainfall intensity based newline on a four year
measurement in a high Alpine rock wall (Reintal, German Alps). Nat hazard earth sys 9, 1425-1432..
https://doi.org/10.5194/nhess-9-1425-2009

Krautblatter, M., Moore, J.R., 2014. Rock slope instability and erosion: toward improved process understanding. Earth Surf Proc
Land 39, 1273-1278.

Kromer, R., Walton, G., Gray, B., Lato, M., 2019. Development and Optimization of an Automated Fixed-Location Time Lapse
Photogrammetric Rock Slope Monitoring System. Remote Sens-Basel11, 1890.. https://doi.org/10.3390/rs11161890

Lazar, A., Beguž, T., Vulič, M., 2018. Monitoring of the Belca rockfall. Acta Geotechnica Slovenica 15, 2-15..
https://doi.org/10.18690/actageotechslov.15.2.2-15.2018

Li, A., Xu, N., Dai, F., Gu, G., Hu, Z., Liu, Y., 2018. Stability analysis and failure mechanism of the steeply inclined bedded rock
masses surrounding a large underground opening. Tunn Undergr Sp Tech 77, 45-58.. https://doi.org/10.1016/j.tust.2018.03.023

Loew, S., GISCHIG, V., WILLENBERG, H., ALPIGER, A., MOORE, J.R., 2012. 24 Randa: Kinematics and driving mechanisms
of a large complex rockslide. Landslides: Types, Mechanisms and Modeling 297-309.

Loew, S., Gschwind, S., Gischig, V., Keller-Signer, A., Valent, G., 2017. Monitoring and early warning of the 2012 Preonzo
catastrophic rockslope failure. Landslides 14, 141-154.. https://doi.org/10.1007/s10346-016-0701-y

Magnin, F., Deline, P., Ravanel, L., Noetzli, J., Pogliotti, P., 2015. Thermal characteristics of permafrost in the steep alpine rock
walls of the Aiguille du Midi (Mont Blanc Massif, 3842 m a.s.l). The Cryosphere 9, 109-121.. https://doi.org/10.5194/tc-9-109-2015

Macciotta, R., Martin, C.D., Edwards, T., Cruden, D.M., Keegan, T., 2015. Quantifying weather conditions for rock fall hazard
management. Georisk 9, 171-186.

Magnin, F., Krautblatter, M., Deline, P., Ravanel, L., Malet, E., Bevington, A., 2015. Determination of warm, sensitive permafrost
areas in near-vertical rockwalls and evaluation of distributed models by electrical resistivity tomography. J Geophys Res-Earth
120, 745-762.. https://doi.org/10.1002/2014JF003351

Ma, C., Li, T., Zhang, H., 2020. Microseismic and precursor analysis of high-stress hazards in tunnels: A case comparison of rockburst and fall of ground. Eng Geol 265, 105435.. https://doi.org/10.1016/j.enggeo.2019.105435

Marmoni, G.M., Fiorucci, M., Grechi, G., Martino, S., 2020. Modelling of thermo-mechanical effects in a rock quarry wall induced by near-surface temperature fluctuations. Int J Rock Mech Min 134.. https://doi.org/https://doi.org/10.1016/j.ijrmms.2020.104440

Matano, F., Pignalosa, A., Marino, E., Esposito, G., Caccavale, M., Caputo, T.), Sacchi, M., Somma, R., Troise, C., De Natale, G., 2015. Laser Scanning Application for Geostructural analysis of Tuffaceous Coastal Cliffs: the case of Punta Epitaffio, Pozzuoli Bay, Italy. Eur J Remote Sens48, 615-637.. https://doi.org/10.5721/EuJRS20154834

Matsuoka, N., 2008. Frost weathering and rockwall erosion in the southeastern Swiss Alps: Long-term (1994–2006) observations. Geomorphology (Amsterdam) 99, 353-368.. https://doi.org/10.1016/j.geomorph.2007.11.013

Matsuoka, N., 2019. A multi-method monitoring of timing, magnitude and origin of rockfall activity in the Japanese Alps. Geomorphology (Amsterdam) 336, 65-76.. https://doi.org/10.1016/j.geomorph.2019.03.023

Pappalardo, G., Mineo, S., Zampelli, S.P., Cubito, A., Calcaterra, D., 2016. InfraRed Thermography proposed for the estimation of the Cooling Rate Index in the remote survey of rock masses. Int J Rock Mech Min (1997) 83, 182-196.. https://doi.org/10.1016/j.ijrmms.2016.01.010

Nishii, R., Matsuoka, N., 2010. Monitoring rapid head scarp movement in an alpine rockslide. Eng Geol 115, 49-57.. https://doi.org/10.1016/j.enggeo.2010.06.014

Noetzli, J., Pellet, C., 2020. 20 years of mountain permafrost monitoring in the Swiss Alps: key results and major challenges, in: Egu General Assembly Conference Abstracts. 2020. p. 10903.

Pappalardo, M., D'Olivo, M., 2019. Testing A Methodology to Assess Fluctuations of Coastal Rocks Surface Temperature. J Mar Sci Eng 7, 315.. https://doi.org/10.3390/jmse7090315

Pasten, C., M. García, M., Cortes, D.D., 2015. Physical and numerical modelling of the thermally induced wedging mechanism. Geotech Lett 5, 186-190.

Pratt, C., Macciotta, R., Hendry, M., 2019. Quantitative relationship between weather seasonality and rock fall occurrences north of Hope, BC, Canada. Bulletin of Eng Geol and the Environment 78, 3239-3251.. https://doi.org/10.1007/s10064-018-1358-7

Racek, O., Blahůt, J., Hartvich, F., 2021. Monitoring of thermoelastic wave within a rock mass coupling information from IR camera and crack meters: a 24-hour experiment on "Branická skála" Rock in Prague, Czechia, in: Understanding And Reducing Landslide Disaster Risk: Volume 3 Monitoring And Early Warning. Springer International Publishing, Cham.

Racek, J., 2020. Use of rock mass classifications for rock fall susceptibility analysis in the conditions of the Bohemian Massif (Bachelor thesis). Praha.

Ravanel, L., Magnin, F., Deline, P., 2017. Impacts of the 2003 and 2015 summer heatwaves on permafrost-affected rock-walls in the Mont Blanc massif. Sci total environ 609, 132-143.. https://doi.org/10.1016/j.scitotenv.2017.07.055

Reiterer, A., Huber, N.B., Bauer, A., 2010. Image-based point detec-tion and matching in a geo-monitoring system.. Allg. Verm.-Nachr. 117, 129–139.

Riquelme, A., Abelian, A., Tomas, R., Jaboyedoff, M., 2014. A new approach for semi-automatic rock mass joints recognition from 3D point clouds. Comput geos 68, 38-52.. https://doi.org/10.1016/j.cageo.2014.03.014

Sarro, R., Riquelme, A., Carlos Garcia-Davalillo, J., Maria Mateos, R., Tomas, R., Luis Pastor, J., Cano, M., Herrera, G., 2018. Rockfall Simulation Based on UAV Photogrammetry Data Obtained during an Emergency Declaration: Application at a Cultural Heritage Site. Remote Sens-Basel10, 1923.. https://doi.org/10.3390/rs10121923

Sass, O., Oberlechner, M., 2012. Is climate change causing increased rockfall frequency in Austria? Nat Hazard Earth Sys 12, 3209-3216.. https://doi.org/10.5194/nhess-12-3209-2012

Scaioni, M., Marsella, M., Crosetto, M., Tornatore, V., Wang, J., 2018. Geodetic and Remote-Sensing Sensors for Dam Deformation Monitoring. Sensors 18, 3682.. https://doi.org/10.3390/s18113682

Saez Blázquez, C., Farfan Martin, A., Martin Nieto, I., Carrasco Garcia, P., Sanchez Perez, L.S., Gonzalez Aguilera, D., 2017. Thermal conductivity map of the Avila region (Spain) based on thermal conductivity measurements of different rock and soil samples. Geothermics 65, 60-71.

Selby, M.J., 1980. A rock mass strength classification for geomorphic purposes: with tests from Antarctica and New Zealand. Z Geomorphol 24, 31-51.

Tertium technology, 2019. Gego Crack meter. Pisa Italy.

Thiele, S. Grose, L., Micklethwaite, S., 2018. Compass: A CloudCompare workflow for digital mapping and structural analysis, in: Eguga. p. 5548.

Tripolitsiotis, A., Daskalakis, A., Mertikas, S., Hristopulos, D., Agioutantis, Z.,, Partsinevelos, P., 2015. Detection of small-scale rockfall incidents using their seismic signature.. Third International Conference on Remote Sens-Baseland Geoinformation of the Environment 9535, 1-9.

Vasile, M., Vespremeanu-Stroe, A., 2017. Thermal weathering of granite spheroidal boulders in a dry-temperate climate, Northern Dobrogea, Romania. Earth Surf Proc Land 42, 259-271.. https://doi.org/10.1002/esp.3984

Vaziri, A., Moore, L., Ali, H., 2010. Monitoring systems for warning impending failures in slopes and open pit mines. Nat Hazards 55, 501-512.. https://doi.org/10.1007/s11069-010-9542-5

Vespremeanu-Stroe, A., Vasile, M., 2010. Rock Surface Freeze-Thaw and Thermal Stress Assessment in two Extreme Mountain Massifs: Bucegi and Măcin Mts. Revista de Geomorfologie 12.

Vonder Mühll, D., Noetzli, J., Roer, I., 2008. PERMOS–A comprehensive monitoring network of mountain permafrost in the Swiss Alps 1869-1874.

Viles, H., 2013. Linking weathering and rock slope instability: non-linear perspectives. Earth Surf Proc Land 38, 62-70.. https://doi.org/10.1002/esp.3294

Warren, K., Eppes, M.-C., Swami, S., Garbini, J., Putkonen, J., 2013. Automated field detection of rock fracturing, microclimate, and diurnal rock temperature and strain fields. Geosci Instrum Meth 2, 275-288.. https://doi.org/10.5194/gi-2-275-2013

Weber, S., Beutel, J., Faillettaz, J., Hasler, A., Krautblatter, M., Vieli, A., 2017. Quantifying irreversible movement in steep, fractured bedrock permafrost on Matterhorn (CH). Cryosphere 11, 567-583.. https://doi.org/10.5194/tc-11-567-2017

Weber, S., Beutel, J., Faillettaz, J., Meyer, M., Vieli, A., 2018. Acoustic and micro-seismic signal of rockfall on Matterhorn., in: 5Th European Conference On Permafrost, Book Of Abstracts. Laboratoire EDYTEM, Université de Savoie Mont-Blanc, pp. 944-945.

Weigand, M., Wagner, F.M., Limbrock, J.K., Hilbich, C., Hauck, C., Kemna, A., 2020. A monitoring system for spatiotemporal electrical self-potential measurements in cryospheric environments. Geosci Instrum Meth9, 317-336.. https://doi.org/10.5194/gi-9-317-2020

Westoby, M.J., Brasington, J., Glasser, N.F., Hambrey, M.J., Reynolds, J.M., 2012. 'Structure-from-Motion' photogrammetry: A low-cost, effective tool for geoscience applications. Geomorphology (Amsterdam) 179, 300-314.. https://doi.org/10.1016/j.geomorph.2012.08.021

705 Yan, Y., Li, T., Liu, J., Wang, W., Su, Q., 2019. Monitoring and early warning method for a rockfall along railways based on vibration signal characteristics. Sci Rep-UK9, 6606-6606.. https://doi.org/10.1038/s41598-019-43146-1

Yavasoglu, H., Alkan, M.N., Bilgi, S., Alkan, O., 2020. Monitoring aseismic creep trends in the İsmetpaşa and Destek segments throughout the North Anatolian Fault (NAF) with a large-scale GPS network. Geosci Instrum Meth 9, 25-40.. https://doi.org/10.5194/gi-9-25-2020

710 Zangerl, C., Eberhardt, E., Perzlmaier, S., 2010. Kinematic behaviour and velocity characteristics of a complex deep-seated crystalline rockslide system in relation to its interaction with a dam reservoir. Eng Geol 112, 53-67.. https://doi.org/10.1016/j.enggeo.2010.01.001

FIEDLER: Elektronika pro ekologii [WWW Document], 2020.. URL https://www.fiedler.company/ (accessed 09.21.2020).

Zhang, F., Zhao, J., Hu, D., Skoczylas, F., Shao, J., 2018. Laboratory Investigation on Physical and Mechanical Properties of

715 Granite After Heating and Water-Cooling Treatment. Rock Mech Rock Eng 51, 677-694.. https://doi.org/10.1007/s00603-017-1350-8